available at www.sciencedirect.com

SCIENCE DIRECT®

journal homepage: www.elsevier.com/locate/biochempharm

# Structure activity and molecular modeling analyses of ribose- and base-modified uridine 5′-triphosphate analogues at the human $P2Y_2$ and $P2Y_4$ receptors

*Kenneth A. Jacobson* [a,*], *Stefano Costanzi* [b], *Andrei A. Ivanov* [a], *Susanna Tchilibon* [a], *Pedro Besada* [a], *Zhan-Guo Gao* [a], *Savitri Maddileti* [c], *T. Kendall Harden* [c]

[a] *Molecular Recognition Section, Laboratory of Bioorganic Chemistry, National Institute of Diabetes and Digestive and Kidney Diseases, National Institutes of Health, Bethesda, MD 20892, USA*

[b] *Computational Chemistry Core Laboratory, National Institute of Diabetes and Digestive and Kidney Diseases, National Institutes of Health, Bethesda, MD 20892, USA*

[c] *Department of Pharmacology, University of North Carolina School of Medicine, Chapel Hill, NC 27599, USA*

ARTICLE INFO

*Article history:*
Received 26 September 2005
Accepted 4 November 2005

*Keywords:*
Structure activity relationship
G protein-coupled receptor
Nucleotides
Phospholipase C
Pyrimidines
Homology modeling

*Abbreviations:*
PLC, phospholipase C
HEPES, N-(2-hydroxyethyl)-piperazine-N′-2-ethanesulfonic acid
ATP, adenosine 5′-triphosphate
CTP, cytidine 5′-triphosphate
GTP, guanosine 5′-triphosphate
TM, transmembrane domain
TBAP, tetrabutylammonium dihydrogen phosphate
TEAA, triethylammonium acetate
UDP, uridine 5′-diphosphate
UTP, uridine 5′-triphosphate

ABSTRACT

With the long-term goal of developing receptor subtype-selective high affinity agonists for the uracil nucleotide-activated P2Y receptors we have carried out a series of structure activity and molecular modeling studies of the human $P2Y_2$ and $P2Y_4$ receptors. UTP analogues with substitutions in the 2′-position of the ribose moiety retained capacity to activate both $P2Y_2$ and $P2Y_4$ receptors. Certain of these analogues were equieffective for activation of both receptors whereas 2′-amino-2′-deoxy-UTP exhibited higher potency for the $P2Y_2$ receptor and 2′-azido-UTP exhibited higher potency for the $P2Y_4$ receptor. 4-Thio substitution of the uracil base resulted in a UTP analogue with increased potency relative to UTP for activation of both the $P2Y_2$ and $P2Y_4$ receptors. In contrast, 2-thio substitution and halo- or alkyl substitution in the 5-position of the uracil base resulted in molecules that were 3–30-fold more potent at the $P2Y_2$ receptor than $P2Y_4$ receptor. 6-Aza-UTP was a $P2Y_2$ receptor agonist that exhibited no activity at the $P2Y_4$ receptor. Stereoisomers of UTPαS and 2′-deoxy-UTPαS were more potent at the $P2Y_2$ than $P2Y_4$ receptor, and the R-configuration was favored at both receptors. Molecular docking studies revealed that the binding mode of UTP is similar for both the $P2Y_2$ and $P2Y_4$ receptor binding pockets with the most prominent dissimilarities of the two receptors located in the second transmembrane domain (V90 in the $P2Y_2$ receptor and I92 in the $P2Y_4$ receptor) and the second extracellular loop (T182 in the $P2Y_2$ receptor and L184 in the $P2Y_4$ receptor). In summary, this work reveals substitutions in UTP that differentially affect agonist activity at $P2Y_2$ versus $P2Y_4$ receptors and in combination with molecular modeling studies should lead to chemical synthesis of new receptor subtype-selective drugs.



* *Corresponding author*. Tel.: +1 301 496 9024; fax: +1 301 480 8422.
*E-mail address:* kajacobs@helix.nih.gov (K.A. Jacobson).

0006-2952/$ – see front matter © 2005 Elsevier Inc. All rights reserved.
doi:10.1016/j.bcp.2005.11.010

## 1. Introduction

Pharmacological effects of UTP (uridine 5′-triphosphate) and other uracil nucleotides on second messenger signaling pathways and on various tissue responses provided the initial indications of the existence of cell surface receptors that specifically recognize extracellular pyrimidines [1,2]. This concept was confirmed and extended over the past decade with the cloning of three different G protein-coupled receptors, the $P2Y_2$, $P2Y_4$ and $P2Y_6$ receptors [3–6] that are activated by uracil nucleotides, and by the direct demonstration of regulated release of UTP from a variety of cell types [7,8].

The $P2Y_2$ receptor is activated equipotently by both UTP and ATP (adenosine 5′-triphosphate) and is distributed in a broad range of tissues. For example, this receptor plays important physiological roles in epithelial cells of the lung, gastrointestinal tract, eye, and other tissues [9,10]. The human $P2Y_4$ receptor is selectively activated by UTP, and ATP is a potent competitive antagonist at this receptor [11]. However, the $P2Y_4$ receptor of several other species is activated by both UTP and ATP [11–13], and therefore, it has proven difficult to differentiate the $P2Y_4$ receptor from the $P2Y_2$ receptor on the basis of its cognate agonists in, for example, rat and mouse tissues. The $P2Y_6$ receptor is selectively activated by UDP (uridine 5′-diphosphate), and UTP is a weak agonist or inactive at this receptor [6,14].

The existence of three different G protein-coupled receptors that recognize uracil nucleotides has made difficult the pharmacological characterization or selective activation of these receptors in native tissues. As has proved to be the case with the P2Y receptors, i.e. $P2Y_1$, $P2Y_{11}$, $P2Y_{12}$, and $P2Y_{13}$ receptors, that are activated by adenine nucleotides, the metabolism and interconversion of extracellular nucleotides add complexities to the study of uracil nucleotide-activated receptors in native tissues [15]. For example, the ectonucleoside triphosphate diphosphohydrolase, NTPDase2, converts extracellular UTP to UDP [16], whereas ectonucleoside diphosphokinase forms UTP from UDP with the transfer of the γ-phosphate from ATP [17].

Drugs that selectively activate or block the uracil nucleotide-activated P2Y receptors would provide armamentaria for circumvention of some of the problems inherent in the study of these physiologically important signaling proteins. However, receptor subtype-selective agonists or antagonists are not available for the uracil nucleotide-activated P2Y receptors [18]. Therefore, we have undertaken a series of pharmacological studies designed to systematically evaluate the effects of various modifications of the UTP structure on the capacity of analogues to activate the UTP-activated $P2Y_2$ and $P2Y_4$ receptors. Since UTP activates the human $P2Y_2$ and $P2Y_4$ receptors with similar potencies, our first goal is to identify substitutions in UTP analogues that differentially affect activity at either of these receptors. Conversely, identification of partial agonists at these receptors would open a path to synthesis of selective high affinity antagonists of the UTP-activated P2Y receptors in a manner similar to the approach we have followed to identify a subnanomolar affinity antagonist for the ADP-activated $P2Y_1$ receptor [19–21]. The results reveal encouraging progress in the first of these goals. We also conducted docking studies with rhodopsin-based homology models of the $P2Y_2$ and $P2Y_4$ receptors with the goal of extending insight gained from the empirical structure activity studies to predict optimized structures that will be pursued by application of new molecular syntheses. The combination of these structure activity analyses and molecular modeling studies provides resolution of key differences in the ligand binding pockets of the $P2Y_2$ versus $P2Y_4$ receptor that will be of heuristic importance for future ligand development.

## 2. Materials and methods

### 2.1. Reagents

2′-Ara-fluoro-2′-deoxyuridine (**25**) was purchased from R.I. Chemical, Inc. (Orange, CA). All other reagents and solvents were purchased from Sigma–Aldrich (St. Louis, MO).

### 2.2. Uracil nucleotide analogues

Most of the nucleotide analogues studied (compounds **5–10**, **12–17**, and **20**) were purchased from TriLink Biotechnologies (San Diego, CA). Compound **19** was custom synthesized by TriLink Biotechnologies and was the gift of Dr. Victor Marquez, NCI, Frederick, MD. Compounds **1–4** and 3-methyluridine (**26**) were purchased from Sigma (St. Louis, MO). Compounds **21–24** were manufactured by Axxora (San Diego, CA)/Biolog Life Science Inst. (Bremen, Germany).

### 2.3. Chemical synthesis

#### 2.3.1. Chemical methods

Methods used to prepare compounds **11** and **18** are depicted schematically in Fig. 1. $^1$H NMR spectra were obtained with a Varian Gemini 300 spectrometer using $D_2O$ as a solvent. The chemical shifts are expressed as relative ppm from HOD (4.78 ppm). $^{31}$P NMR spectra were recorded at room temperature by use of Varian XL 300 spectrometer (121.42 MHz); orthophosphoric acid (85%) was used as an external standard. Purity of compounds was checked using a Hewlett-Packard 1100 HPLC equipped with a Luna 5μ RP-C18(2) analytical column (250 mm × 4.6 mm; Phenomenex, Torrance, CA). System A—linear gradient solvent system: 5 mM TBAP-$CH_3CN$ from 80:20 to 40:60 in 20 min, then isocratic for 2 min; the flow rate was 1 mL/min. System B—linear gradient solvent system: 10 mM TEAA-$CH_3CN$ from 100:0 to 90:10 in 20 min, then isocratic for 2 min; the flow rate was 1 mL/min. Peaks were detected by UV absorption with a diode array detector. All derivatives tested for biological activity showed >99% purity in the HPLC systems. High-resolution mass measurements were performed on Micromass/Waters LCT Premier Electrospray Time of Flight (TOF) mass spectrometer coupled with a Waters HPLC system. Purification of the nucleotide analogues for biological testing was carried out on (diethylamino)ethyl (DEAE)-A25 Sephadex columns with a linear gradient (0.01–0.5 M) of 0.5 M ammonium bicarbonate as the mobile phase. Compounds **27** and **28** were additionally purified by HPLC using system C (10 mM TEAA-$CH_3CN$ from 100:0 to 90:10 in 30 min, then isocratic for 2 min; the flow rate was 2 mL/min)

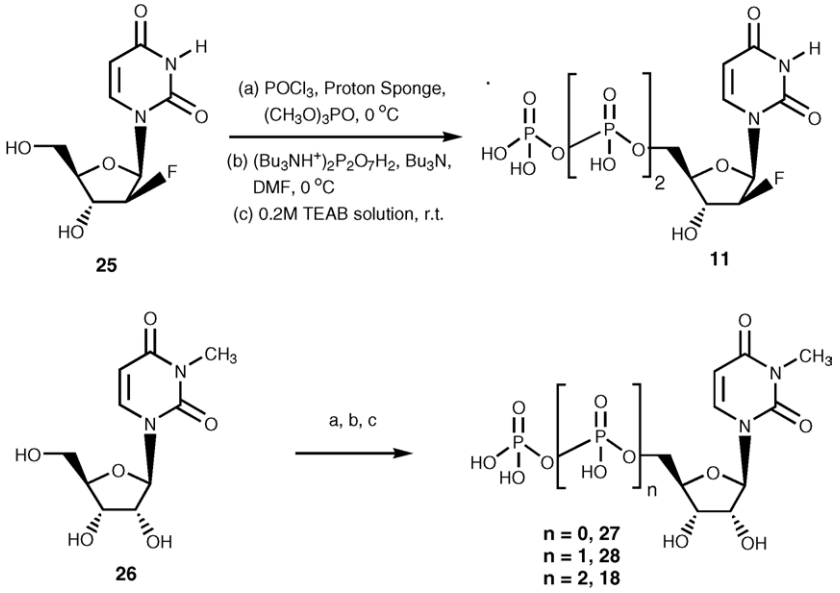


**Fig. 1 – Synthetic methods for the preparation of compounds 11 and 18.**

with a Luna 5μ RP-C18(2) semipreparative column (250 mm × 10.0 mm; Phenomenex, Torrance, CA).

#### 2.3.2. *General procedure for preparation of nucleoside 5′-triphosphate (compound 18)*

3-Methyluridine (**26**) (25 mg, 0.10 mmol) and Proton Sponge (31 mg, 0.15 mmol) were dried for several hours in high vacuum and then dissolved in trimethyl phosphate (1 mL). After cooling the solution at 0 °C, phosphorous oxychloride (0.02 mL, 0.19 mmol) was added. The mixture reaction was stirred at 0 °C for 2 h. A solution of tributylammonium pyrophosphate (303 mg, 0.64 mmol) and tributylamine (0.09 mL, 0.39 mmol) in DMF (1 mL) was added and stirring was continued at 0 °C for additional 20 min. Five milliliters of 0.2 M triethylammonium bicarbonate (TEAB) solution was added, and the reaction mixture was stirred at room temperature for 45 min. Analysis of the reaction mixture by analytical HPLC (System A) indicated the formation of three compounds, the corresponding nucleotide mono-, di-, and triphosphates. The mixture was subsequently frozen and lyophilized, and the residue was purified by Sephadex-DEAE A-25 resin ion-exchange column chromatography and when was necessary (compounds **27** and **28**) by semipreparative HPLC as described above. The corresponding nucleotide mono-, di-, and triphosphates were collected, frozen, and lyophilized as the triethylammonium or ammonium salts. (2′*R*,3′*R*,4′*S*,5′*R*)-1-(3′,4′-dihydroxy-5′-phosphoryloxymethyl-tetrahydro-furan-2′-yl)-3-methyl-1H-pyrimidine-2,4-dione, triethylammonium salt (**27**) was obtained as a white solid (6 mg, 11%). $^1$H NMR ($D_2O$) $\delta$ 8.06 (d, $J$ = 8.4 Hz, 1H), 6.04 (d, $J$ = 8.1 Hz, 1H), 6.02 (d, $J$ = 4.2 Hz, 1H), 4.37 (m, 2H), 4.28 (m, 1H), 4.07 (m, 2H), 3.30 (s, 3H); $^{31}$P NMR ($D_2O$) $\delta$ 1.88; HRMS *m/z* found 337.0404 $(M - H^+)^-$. $C_{10}H_{14}N_2O_9P$ requires 337.0437; HPLC (System A) 7.6 min (99%), (System B) 11.5 min (99%). (2′*R*,3′*R*,4′*S*,5′*R*)-1-(3′,4′-dihydroxy-5′-diphosphoryloxymethyl-tetrahydro-furan-2′-yl)-3-methyl-1H-pyrimidine-2,4-dione, triethylammonium salt (**28**) was obtained as a white solid (1 mg, 1%). $^1$H NMR ($D_2O$) $\delta$ 8.01 (d, $J$ = 7.8 Hz, 1H), 6.05 (d, $J$ = 8.1 Hz, 1H), 6.01 (d, $J$ = 3.6 Hz, 1H), 4.41 (m, 2H), 4.27 (m, 3H), 3.31 (s, 3H); $^{31}$P NMR ($D_2O$) $\delta$ −8.68, −11.32 (d, $J$ = 21.4 Hz); HRMS *m/z* found 417.0116 $(M - H^+)^-$. $C_{10}H_{15}N_2O_{12}P_2$ requires 417.0100; HPLC (System A) 14.3 min (99%), (System B) 12.4 min (99%). (2′*R*,3′*R*,4′*S*,5′*R*)-1-(3′,4′-dihydroxy-5′-triphosphoryloxymethyl-tetrahydro-furan-2′-yl)-3-methyl-1H-pyrimidine-2,4-dione, ammonium salt (**18**) was obtained as a white solid (8 mg, 15%). $^1$H NMR ($D_2O$) $\delta$ 7.98 (d, $J$ = 8.1 Hz, 1H), 6.02 (m, 2H), 4.44 (m, 1H), 4.40 (m, 1H), 4.28 (m, 3H), 3.29 (s, 3H); $^{31}$P NMR ($D_2O$) $\delta$ −6.64 (d, $J$ = 20.2 Hz), −10.88 (d, $J$ = 19.5 Hz), −21.91 (t, $J$ = 20.2 Hz); HRMS *m/z* found 496.9750 $(M - H^+)^-$. $C_{10}H_{16}N_2O_{15}P_3$ requires 496.9764; HPLC (System A) 18.3 min (99%), (System B) 13.5 min (99%).

(2′*R*,3′*S*,4′*S*,5′*R*)-1-(3′-Fluoro-4′-hydroxy-5′-triphosphorylox-ymethyl-tetrahydro-furan-2′-yl)-1H-pyrimidine-2,4-dione, ammonium salt (**11**). Compound **11** (29 mg, 26%) was obtained as a white solid from 2′-ara-fluoro-2′-deoxyuridine (**25**) following the general procedure for **18**. $^1$H NMR ($D_2O$) $\delta$ 7.93 (d, $J$ = 8.1 Hz, 1H), 6.34 (d, $J$ = 15.6 Hz, 1H), 5.94 (d, $J$ = 8.1 Hz, 1H), 5.24 (d, $J$ = 51.6 Hz, 1H), 4.60 (d, $J$ = 19.5 Hz, 1H), 4.25 (m, 3H); $^{31}$P NMR ($D_2O$) $\delta$ −9.86, −11.46 (d, $J$ = 19.6 Hz), −23.05; HRMS *m/z* found 484.9576 $(M - H^+)^-$. $C_9H_{13}N_2O_{14}FP_3$ requires 484.9564; HPLC (System A) 19.0 min (99%), (System B) 11.6 min (99%).

### 2.4. *Assay of P2Y$_2$ and P2Y$_4$ receptor-stimulated phospholipase C activity*

Stable cell lines expressing the human $P2Y_2$ receptor or the human $P2Y_4$ receptor in 1321N1 human astrocytoma cells were generated as previously described in detail [14]. Agonist-induced [$^3$H]inositol phosphate production was measured in 1321N1 cells grown to confluence on 48-well plates. Twelve hours before the assay, the inositol lipid pool of the cells was radiolabeled by incubation in 200 μL of serum-free inositol-free Dulbecco's modified Eagle's medium, containing 0.4 μCi

of *myo*-[$^3$H]inositol. No changes of medium were made subsequent to the addition of [$^3$H]inositol. On the day of the assay, cells were challenged with 50 μL of the five-fold concentrated solution of receptor agonists in 200 mM Hepes, pH 7.3, containing 50 mM LiCl for 20 min at 37 °C. Incubations were terminated by aspiration of the drug-containing medium and addition of 450 μL of ice-cold 50 mM formic acid. After 15 min at 4 °C, samples were neutralized with 150 μL of 150 mM $NH_4OH$. [$^3$H]Inositol phosphates were isolated by ion exchange chromatography on Dowex AG 1-X8 columns as previously described [22].

### 2.5. Data analyses

Agonist potencies ($EC_{50}$ values) were obtained from concentration–response curves by non-linear regression analysis using the GraphPad software package Prism (GraphPad, San Diego, CA). All experiments were performed in triplicate assays and repeated at least three times. The results are presented as mean ± S.E.M. from multiple experiments or in the case of concentration effect curves from a single experiment carried out with triplicate assays that were representative of results from multiple experiments.

### 2.6. Reconstruction of the binding pocket model

The reconstruction of the $P2Y_2$ and $P2Y_4$ receptors around UTP was performed with the InducedFit module of the Prime 1.2 homology modeling program (Schrödinger, LLC). The calculation was restricted to the residues located within 5 Å of the ligand.

### 2.7. Conformational analysis of UTP inside the putative binding pocket

A conformational analysis of UTP in the binding pockets of the $P2Y_2$ and $P2Y_4$ receptors was performed by means of the mixed MCMM/LMCS sampling method as implemented in MacroModel 9.0 [23] (Schrödinger, LLC). The approach combines the Monte Carlo Multiple Minimum (MCMM) [24] and the low-mode conformational search (LMCS) [25]. All of the rotatable bonds of the ligand, as well as the ligand itself as a single body, were subjected to Monte Carlo driven rotations and translations during the conformational search. The search was performed on the ligand and the residues located within 5 Å of the ligand, while the remaining residues were conformationally frozen. The calculations were conducted with the MMFFs force field [26], using water as implicit solvent (GB/SA model [27] as implemented in MacroModel [23]) and a molecular dielectric constant of 1. The Polak-Ribier Conjugate Gradient was used for the energy minimizations with a convergence threshold of 0.05 kJ/mol/Å.

## 3. Results

### 3.1. Chemical synthesis

Synthetic methods for the preparation of nucleoside 5′-triphosphate derivatives **11** and **18** from the nucleosides of **25** and **26**, respectively, are shown in Fig. 1. The classical phosphorous oxychloride method was used for the synthesis of both derivatives [28,29]. The 5′-mono (**27**) and diphosphate (**28**) derivatives of **26** were also isolated as side products.

### 3.2. Pharmacological assays and structure activity relationships

The human $P2Y_2$ and $P2Y_4$ receptors were stably expressed in 1321N1 human astrocytoma cells using retroviral vectors as previously described [14]. Agonist-promoted activation of phospholipase C (PLC) was assessed in these two stable cell lines by quantification of the accumulation of [$^3$H]inositol phosphates as described in Section 2. UTP markedly stimulated [$^3$H]inositol phosphate accumulation to similar levels in $P2Y_2$ versus $P2Y_4$ receptor-expressing cells. Similar $EC_{50}$ values also were observed for UTP (**1**) for activation of the two receptors (Fig. 2 and Table 1). ATP (**2**) was two-fold less potent than UTP at the human $P2Y_2$ receptor, and CTP (**3a**) and GTP (**3b**) were only weakly active at this subtype. Both nucleotides were previously shown to be antagonists at the human $P2Y_4$ receptor [11].

Given the similar activities of UTP at the $P2Y_2$ versus $P2Y_4$ receptor, we compared the activities of a series of ribose-

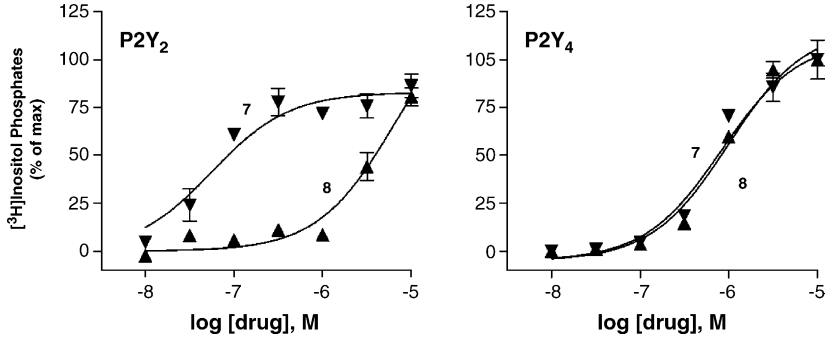


**Fig. 2 – Activation of the human $P2Y_2$ (left panel), and $P2Y_4$ (right panel) receptors by ribose-modified uracil 2′-deoxynucleotide analogues containing 2′-amino (*7*) (▼) and 2′-azido (*8*) (▲) functionality. PLC activity was measured as described in Section 3.2 in 1321N1 human astrocytoma cells stably expressing the human P2Y receptors. The data are the means of triplicate determinations and are representative of results obtained in at least three separate experiments with each analog.**

**Table 1 – In vitro pharmacological data for UTP (1) and its analogues in the stimulation of PLC at recombinant human $P2Y_2$ and $P2Y_4$ receptors expressed in astrocytoma cells**

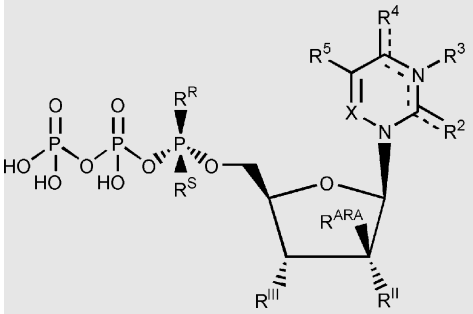

Compounds **4** - **19**, **21** - **24**

$R^2$, $R^4$ = O, unless noted

$R^3$, $R^5$, $R^{ARA}$ = H, unless noted

$R^{II}$, $R^{III}$ = OH, unless noted

$R^R$, $R^S$ = =O, unless noted

X = CH, unless noted

| Compound | Modification | Structure | $EC_{50}$ at $hP2Y_2$ receptor (μM)[a] | Relative to UTP | $EC_{50}$ at $hP2Y_4$ receptor (μM)[a] | Relative to UTP |
|---|---|---|---|---|---|---|
| Native ribonucleoside-5′-triphosphates | | | | | | |
| **1** UTP | | | 0.049 ± 0.012 | 1 | 0.073 ± 0.02 | 1 |
| **2** ATP | | | 0.085 ± 0.012 | 1.7 | Antagonist[b] | |
| **3a** CTP | | | 5.63 ± 0.30 | 110 | Antagonist[b] | |
| **3b** GTP | | | 2.64 ± 0.30 | 54 | 6.59[b] | 90 |
| Ribose-modified UTP analogues | | | | | | |
| **4** | 2′-Deoxy | $R^{II}$ = H | 1.08 ± 0.28 | 22 | 1.9 ± 0.5 | 26 |
| **5** | 2′-Deoxy-2′-methoxy | $R^{II}$ = $OCH_3$ | 14.3 ± 7.7 | 290 | 8.2 ± 2.1 | 110 |
| **6** | 3′-Deoxy-3′-methoxy | $R^{III}$ = $OCH_3$ | NE | >1000 | NE | >1000 |
| **7** | 2′-Amino-2′-deoxy | $R^{II}$ = $NH_2$ | 0.062 ± 0.008 | 1.3 | 1.2 ± 0.3 | 16 |
| **8** | 2′-Azido-2′-deoxy | $R^{II}$ = $N_3$ | 5.0 ± 2.1 | 100 | 1.1 ± 0.1 | 15 |
| **9** | 2′-Deoxy-2′-fluoro | $R^{II}$ = F | 0.78 ± 0.11 | 16 | 0.54 ± 0.14 | 7.4 |
| **10** | Arabino | $R^{II}$ = H, $R^{ARA}$ = OH | 0.087 ± 0.010 | 1.8 | 0.71 ± 0.08 | 9.7 |
| **11** | 2′-Deoxy-arabino-2′-fluoro- | $R^{II}$ = H, $R^{ARA}$ = F | 0.52 ± 0.15 | 11 | 0.52 ± 0.08 | 7.1 |
| Uracil-modified UTP analogues | | | | | | |
| **12** | 5-Bromo | $R^5$ = Br | 0.75 ± 0.1 | 15 | 2.1 ± 0.7 | 29 |
| **13** | 5-Iodo | $R^5$ = I | 0.83 ± 0.1 | 17 | 4.0 ± 1.7 | 55 |
| **14** | 5-Methyl | $R^5$ = $CH_3$ | 0.48 ± 0.1 | 9.8 | 3.9 ± 1.6 | 53 |
| **15** | 2-Thio | $R^2$ = S | 0.035 ± 0.004 | 0.71 | 0.35 ± 0.01 | 4.8 |
| **16** | 4-Thio | $R^4$ = S | 0.026 ± 0.01 | 0.53 | 0.023 ± 0.005 | 0.32 |
| **17** | 6-Aza | X = N | 8.6 ± 3.7 | 180 | NE | >1000 |
| **18** | 3-Methyl | $R^3$ = $CH_3$ | 1.20 ± 0.20 | 24 | 3.4 ± 0.8 | 47 |
| **19** | Zebularine analogue | $R^4$ = H, H | 8.9 ± 0.5 | 180 | NE | >1000 |
| **20** | Pseudouridine | [c] | 0.78 ± 0.5 | 16 | 3.0 ± 0.3 | 41 |
| Phosphate-modified UTP analogues | | | | | | |
| **21** | $R_p$-α-thio | $R^R$ = S | 5.4 ± 1.5 | 110 | 27 ± 5 | 370 |
| **22** | $S_p$-α-thio | $R^S$ = S | 14 ± 5.5 | 290 | 81 ± 8 | 1100 |
| **23** | 2′-Deoxy-$R_p$-α-thio-triphosphate | $R^R$ = S, $R^{II}$ = H | 12.5 ± 6.7 | 260 | NE | >1000 |
| **24** | 2′-Deoxy-$S_p$-α-thio triphosphate | $R^S$ = S $R^{II}$ = H | NE | >1000 | NE | >1000 |

NE: no effect at 10 μM.

[a] Agonist potencies were calculated using a four-parameter logistic equation and the GraphPad software package (GraphPad, San Diego, CA). $EC_{50}$ values (mean ± S.E.) represent the concentration at which 50% of the maximal effect is achieved. $EC_{50}$ is also expressed relative to the value for UTP at each receptor. Relative efficacies (%) were determined by comparison with the effect produced by a maximal effective concentration of reference agonist (UTP) in the same experiment. For all of the nucleotides, except 22 and 23, for which an $EC_{50}$ is reported in this table, ~100% efficacy was achieved.

[b] ATP antagonized the human $P2Y_4$ receptor with a $K_B$ of 0.708 μM. CTP (100 μM) inhibited the response to an $EC_{50}$ concentration of UTP by ~40% [11].

[c] Compound **20** has the following structure:

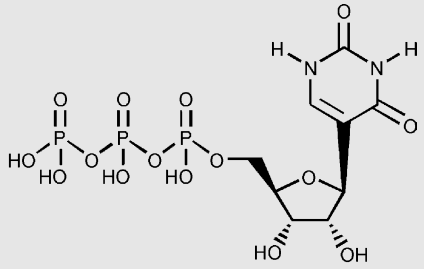

NE - no effect at 10 μM.

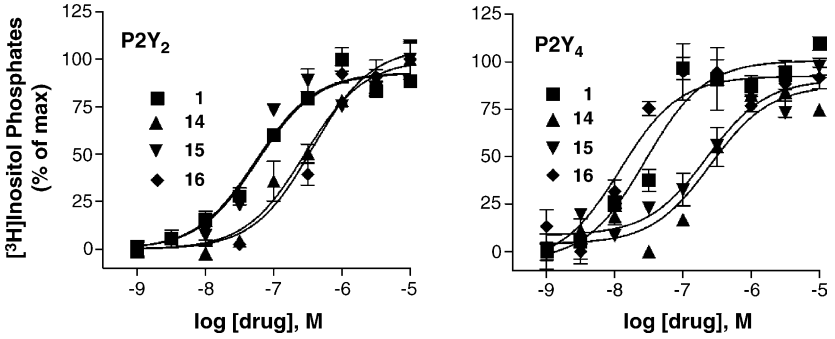


**Fig. 3 – Activation of the human $P2Y_2$ (left panel), and $P2Y_4$ (right panel) receptors by UTP (1) and its base-modified uracil nucleotide analogues having 5-methyl (14), 2-thio (15), and 4-thio (16) substitution. PLC activity was measured as described in Section 3.2 in 1321N1 human astrocytoma cells stably expressing the human P2Y receptors. The data are the means of triplicate determinations and are representative of results obtained in at least three separate experiments with each analog.**

modified UTP analogues (**4**–**11**) for activation of the two receptor types. Although less potent than UTP in most cases, all 2′-substituted molecules retained capacity to maximally stimulate both receptors in the test system used. Whereas similar potencies were observed for the 2′-*O*-methyl-substituted (**5**) and 2′-fluoro-substituted (**9**) molecules at the $P2Y_2$ versus $P2Y_4$ receptors (Table 1), differential effects on potencies at the two receptors were observed with 2′-amino (**7**) and 2′-azido (**8**) substitutions (Fig. 2 and Table 1). That is, the potency of 2′-amino-2′-deoxyuridine-5′-triphosphate (**7**) was unchanged from UTP at the $P2Y_2$ receptor but was 16-fold less at the $P2Y_4$ receptor. Conversely, 2′-azido-substitution in **8** resulted in a greater decrease in potency at the $P2Y_2$ receptor than at the $P2Y_4$ receptor. Interestingly, existence of the 2′-hydroxyl of UTP in the arabino configuration in **10** resulted in a molecule that exhibits similar potency to UTP at the $P2Y_2$ receptor but 10-fold reduced potency at the $P2Y_4$ receptor. The only 3′-substituted molecule, 3′-*O*-methyluridine-5′-triphosphate (**6**), tested was inactive at both $P2Y_2$ and $P2Y_4$ receptors.

Uracil-substituted UTP analogues (**12**–**20**) also were examined. Modification of UTP with a thio moiety in the 4 position in **16** resulted in an analogue that was two-fold and three-fold more potent than UTP at the $P2Y_2$ and $P2Y_4$ receptors, respectively (Fig. 3 and Table 1). In contrast, 2-thio-substitution in **15** resulted in a molecule that was at least as potent as UTP at the $P2Y_2$ receptor and 5-fold less potent at the $P2Y_4$ receptor. Halo- or alkyl substitution in the 5-position of the base (**12**–**14**) resulted in molecules 3–10-fold more potent at the $P2Y_2$ receptor than the $P2Y_4$ receptor. Aza-substitution in the 6-position in **17** decreased potency at the $P2Y_2$ receptor and resulted in an analogue that was inactive at the $P2Y_4$ receptor. A decrease in $P2Y_2$ receptor potency and complete loss of activity at the $P2Y_4$ receptor also occurred with replacement of uracil with a pyrimidinone ring moiety, i.e. zebularine-5′-triphosphate [30]. Conversely, attenuated agonist activity was observed at the $P2Y_2$ and $P2Y_4$ receptors with pseudouridine-5′-triphosphate (**20**), in which the base moiety is replaced with a reoriented uracil ring.

Phosphate side chain modification as phosphothioates was examined in the stereoisomers of UTPαS and 2′-deoxy-UTPαS (**21**–**24**). These phosphate side chain modifications decreased agonist potency by approximately two orders of magnitude. Both stereoisomers of UTPαS (**21**, **22**) were approximately five-fold more potent at the $P2Y_2$ receptor than the $P2Y_4$ receptor (Fig. 4 and Table 1). The R-configuration was favored by both receptors by approximately three-fold over the S-isomer. $R_p$-2′-deoxy-UTPαS (**23**), although displaying a relatively large standard error, was a full agonist at the $P2Y_2$ receptor and inactive at the $P2Y_4$ receptor. $S_p$-2′-deoxy-UTPαS (**24**) was inactive at both the $P2Y_2$ and $P2Y_4$ receptors.

### 3.3. *Flexible docking of UTP into putative binding pockets of the $P2Y_2$ and $P2Y_4$ receptors*

We recently proposed, supported by experimental data, a hypothetical binding mode of nucleotides within P2Y receptors of subgroup A ($P2Y_1$, $P2Y_2$, $P2Y_4$, $P2Y_6$, and $P2Y_{11}$) [31,32]. Briefly, the cognate agonist nucleotide of each of these receptors is accommodated in the cavity defined by the third, sixth, and seventh transmembrane domains (TM) and the second extracellular loop (EL2). The ribose moiety of agonists is located between TM3 and TM7, with the negatively charged phosphate groups pointing toward TM6 and the nucleobase pointing toward TM1 and TM2.

Our previous success in identification of new receptor-selective high affinity agonists and antagonists of the $P2Y_1$ receptor [19–21,33] was driven in part by a close interplay of structure activity analyses, rational new drug syntheses, and molecular modeling of the $P2Y_1$ receptor binding site. Thus, we have carried out new modeling studies as described in Section 2 to further refine insight into the binding pocket of the $P2Y_2$ and $P2Y_4$ receptors. Our previously published binding mode [31,32] was utilized to position UTP in the putative binding pockets of the unoccupied $P2Y_2$ and $P2Y_4$ receptors. These respective binding pockets then were reconstructed around docked UTP by means of homology modeling under conditions that allowed the receptors to adapt to the presence of ligand. We subsequently performed a concerted conformational analysis of UTP and the surrounding residues, exploring simultaneously the flexibility of the ligand and the receptors. To facilitate the comparison among receptors, throughout this

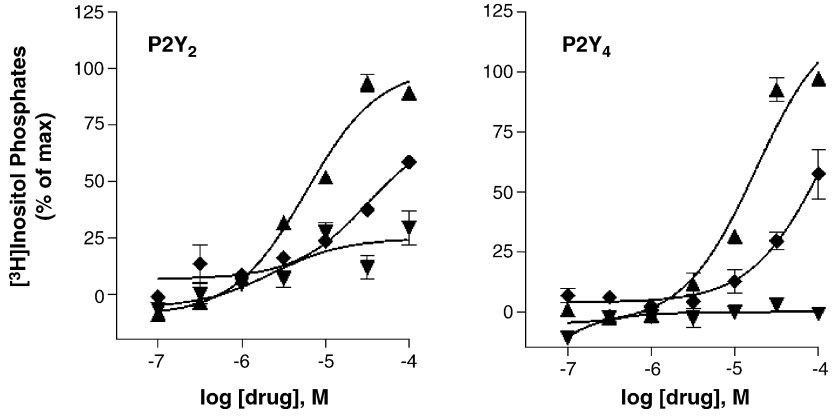


**Fig. 4 – Activation of the human $P2Y_2$ (left panel), and $P2Y_4$ (right panel) receptors by chiral α-phosphothioate uracil nucleotide analogues 21 (▲), 22 (◆), and 23 (▼). PLC activity was measured as described in Section 3.2 in 1321N1 human astrocytoma cells stably expressing the human P2Y receptors. The data are the means of triplicate determinations and are representative of results obtained in three separate experiments.**

paper we use the GPCR residue indexing system, as explained in detail elsewhere [31].

The putative nucleotide binding pockets of the $P2Y_2$ and $P2Y_4$ receptors are highly conserved and, not surprisingly, the results of our docking experiments indicated very similar binding modes of UTP within both receptors (Fig. 5). The most prominent dissimilarities between the putative UTP binding pockets in the $P2Y_2$ and $P2Y_4$ receptors were found in residues located in TM2 (V90(2.61) in the $P2Y_2$ receptor corresponding to I92(2.61) in the $P2Y_4$ receptor) and a residue in EL2 (T182 in the $P2Y_2$ receptor corresponding to L184 in $P2Y_4$ receptor). Both of these non-conserved residues are located in proximity to the uracil moiety of UTP, and their presence results in an apparently smaller binding pocket of the $P2Y_4$ receptor for the cognate agonist.

The docking models suggested other ligand recognition elements. In agreement with observations for the $P2Y_1$ receptor [31,32], the triphosphate moiety of UTP is putatively coordinated by three conserved cationic residues (Fig. 5). These residues, all Arg in $P2Y_2$ and $P2Y_4$ receptors, are located in TM3 (3.29), TM6 (6.55), and TM7 (7.39). A fourth cationic residue located at the 7.36 position is in proximity to the ligand but, consistent with mutagenesis data [34], apparently does not directly interact. The NH at the 3-position of the uracil ring donates an H-bond to a Ser in TM7 (7.43). Alternatively, in other docking poses Ser(7.43) donated an H-bond to the oxygen at the 2-position of the uracil ring. This Ser residue is highly conserved within the P2Y family. Mutagenesis data revealed its fundamental role in the recognition of agonists and antagonists at the $P2Y_1$ receptor, where it is probably involved in the coordination of the adenine base [31].

## 4. Discussion

Results from this study provide the first systematic structure activity analysis designed to distinguish the $P2Y_2$ versus $P2Y_4$ receptor selectivity of base- and ribose-modified analogues of UTP. The UTP receptor selectivity of molecules with phosphate side chain modified UTP, i.e. stereoisomers of UTPαS and 2′-deoxy-UTPαS, also was examined. Thio-substitution at the 4-position increases potency at both $P2Y_2$ and $P2Y_4$ receptors, whereas other base- or ribose-modifications were identified that differentially affect the capacity of analogues to activate the $P2Y_2$ versus $P2Y_4$ receptor. These results lay the groundwork for rational drug synthesis directed at generation of high affinity agonists that selectively activate either the $P2Y_2$ receptor or $P2Y_4$ receptor.

The $P2Y_2$ receptor is broadly distributed in mammalian tissues, and its expression in epithelial cells of the lung, eye, and other tissues make it a potentially important therapeutic target in cystic fibrosis, eye disease, and other pathophysiologies [9,10]. Although the $P2Y_4$ receptor is less prominent than the $P2Y_2$ receptor in mammals, the presence of this signaling protein on neuronal, vascular, and epithelial tissues also makes the $P2Y_4$ receptor a potentially important drug target. Simultaneous expression of $P2Y_2$ and $P2Y_4$ receptors occurs in a number of cell types and tissues. These receptors theoretically can be delineated in human tissues since whereas both UTP and ATP activate the human $P2Y_2$ receptor, only UTP activates the human $P2Y_4$ receptor. However, both of these receptors are potently activated by ATP and UTP in rodents [11–13], and the complexities introduced by metabolism and interconversion of nucleotides also makes pharmacological delineation of the $P2Y_2$ and $P2Y_4$ receptors difficult in human tissues using the natural triphosphate agonists [15].

Few studies have addressed selectivity of synthetic nucleotide analogues at the $P2Y_2$ and $P2Y_4$ receptors, and no systematic comparison of structure activity relationships has been made for the $P2Y_2$ receptor versus $P2Y_4$ receptor using a unified assay system. Certain UTP analogues with substitutions in the 4-position of the base have been reported, and several of these, e.g. 4-*SH* or 4-S-hexyl analogues of UTP, retained potencies similar to UTP at the $P2Y_2$ receptor [35]. To our knowledge the activities of these molecules at the $P2Y_4$ receptor have not been reported. 5-Br-UTP is an agonist at both $P2Y_2$ and $P2Y_4$ receptors, but relative potencies have not been compared simultaneously in the same test system. We

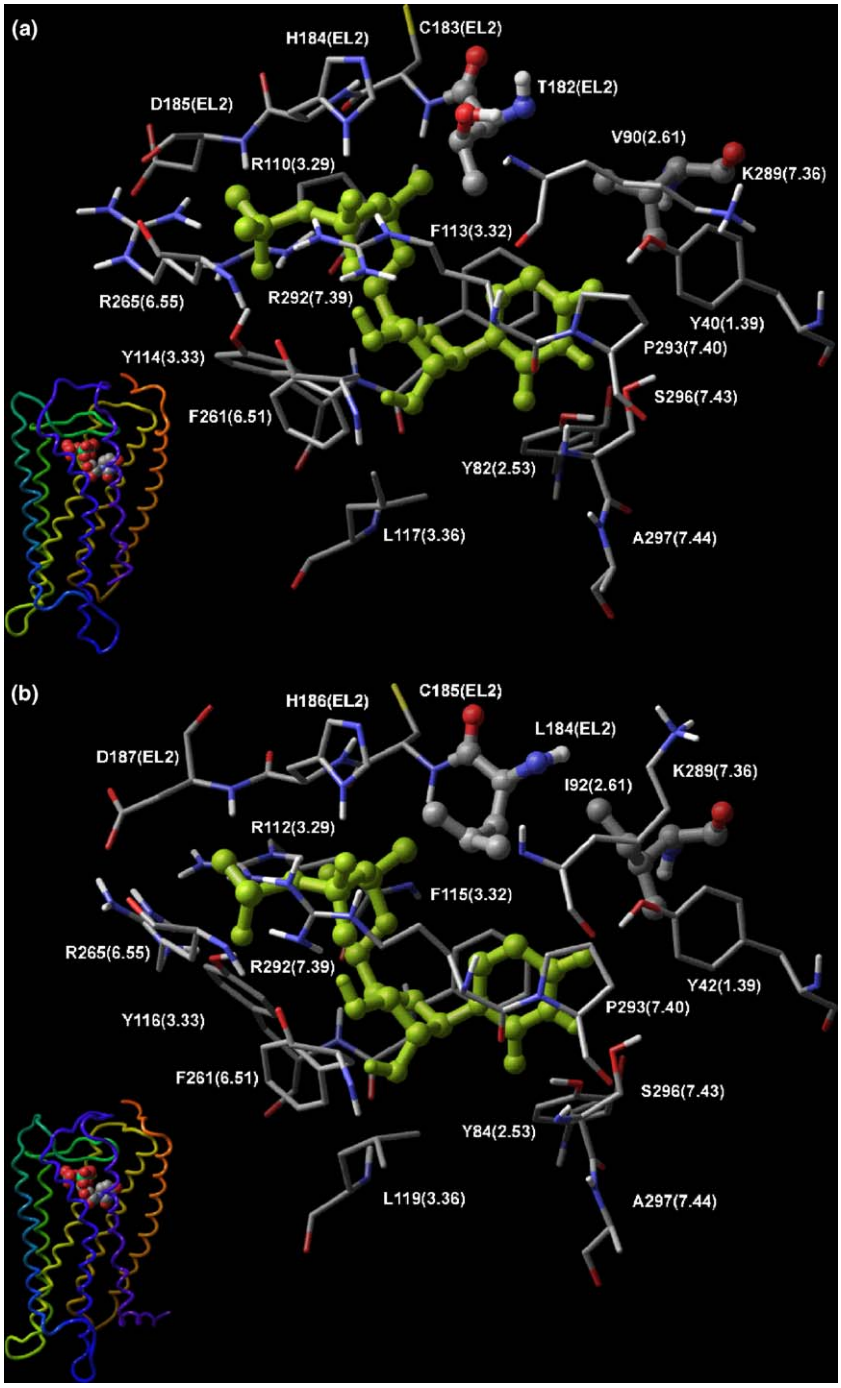


**Fig. 5 – Models of the complexes formed by UTP (*1*) with the $P2Y_2$ (a) and $P2Y_4$ (b) receptors. The nucleotide binding pockets are highly conserved in the two receptors [23]. The only two sites of divergence can be found in two residues located in TM2 and EL2 (represented with balls and sticks) in proximity to the uracil-binding pocket. To the left of each detailed binding site is a schematic representation of the entire receptor structure complexed with UTP. In the tube representations the receptor is colored according to residue positions, with a spectrum of colors that ranges from red (N-terminus) to purple (C-terminus): TM1 is in orange, TM2 in ochre, TM3 in yellow, TM4 in green, TM4 in cyan, TM5 in blue, TM7 in purple.**

previously directly compared at the human $P2Y_2$ and $P2Y_4$ receptors analogues of both UTP and ATP in which the ribose moiety was replaced by a fixed ring (methanocarba) system, i.e. a cyclopentane fused in the Northern confirmation with a cyclopropane ring [33]. (*N*)-Methanocarba UTP was equipotent to UTP at both the $P2Y_2$ and $P2Y_4$ receptors, and this analogue was approximately five-fold more potent at the $P2Y_2$ receptor than the $P2Y_4$ receptor. In contrast, whereas (*N*)-methanocarba-ATP is a very potent agonist at the human $P2Y_2$ receptor, (*N*)-methanocarba-ATP like ATP itself is inactive at the human

$P2Y_4$ receptor. UTPγS is a reasonably potent agonist at both $P2Y_2$ and $P2Y_4$ receptors [36,37]. Receptor activity also is retained in UTP analogues with imido- and methylene-modifications of the phosphate side chain [18]. Finally, both diadenosine and diuridine polyphosphate molecules are agonists at the $P2Y_2$ receptor with the most potent of these reported to be dinucleotides with four phosphates [29]. $Up_4U$ also is a potent $P2Y_4$ receptor agonist.

The current structure activity studies provide encouraging new insight on agonist action at the $P2Y_2$ versus $P2Y_4$ receptors. Certain substitutions, e.g. thio-substitution in the 4-position of the uracil base, resulted in increases in potency at both the $P2Y_2$ and $P2Y_4$ receptors. These increases in potency are explainable on the basis of the favorable interactions that the sulfur atom establishes with hydrophobic residues from TM1, TM7, and EL2 in the binding pockets of both receptors (Fig. 5). These results strongly suggest that relative affinity can be retained or enhanced in future analogues modified in other positions to alter their P2Y receptor subtype-selectivity. The stereoselectivity in recognition of α-thiophosphate analogues of UTP showed a small but consistent preference at both $P2Y_2$ and $P2Y_4$ receptors for the $R_p$ isomer, which is the opposite of the diastereoselectivity found at the $P2Y_1$ receptor [39].

A large number of modifications of the base or ribose moiety resulted in differential changes in the potency of analogues at the two receptors. Several base modifications differentially affected $P2Y_2$ receptor versus $P2Y_4$ receptor selectivity, but in all such cases $P2Y_2$ receptor potency was better retained than activity at the $P2Y_4$ receptor. As presented in Section 3, molecular modeling indicates a larger size for the base-interacting portion of the $P2Y_2$ binding pocket compared to that of the $P2Y_4$ receptor, and the observed enhancement of selectivity, for example, in the 5-substituted analogs is consistent with this predicted difference between the steric bulk tolerance of the $P2Y_2$ receptor versus the $P2Y_4$ receptor.

The observation that introduction of different functional groups in the 2′ position resulted in analogues that favored the $P2Y_2$ receptor in some cases, e.g. 2′-amino, or the $P2Y_4$ receptor in another substitution, e.g. 2′-azido, suggests both subtle differences in the binding pocket of these two receptors and avenues for developing analogues that favor binding to one of these UTP-activated receptors. The 3′-OH is intramolecularly H-bonded to the β-phosphate (Fig. 5) and, according to our molecular dynamics (MD) studies on the $P2Y_6$–UDP complex [38], could be involved in an interaction with the cationic residues, possibly mediated by a water molecule. Therefore, substitutions at this position are likely to be detrimental for activity. Conversely, the 2′-OH apparently does not interact directly with the receptor. Hence, substitutions at this position are likely to be tolerated and can be exploited to modulate the $P2Y_2$/$P2Y_4$ receptor selectivity. The residues that interact directly with the ribose moiety are conserved in the $P2Y_2$ and the $P2Y_4$ receptors (Fig. 5). Thus, the selectivities observed with various 2′-substituted compounds for the $P2Y_2$ or $P2Y_4$ receptors must arise from non-conserved residues located further away from the ligand that indirectly affect the shape of the binding pocket. Prolonged MD simulations of the receptor–ligand complexes in a phospholipid bilayer should reveal these residues.

In summary, these results indicate that agonist potency and $P2Y_2$ versus $P2Y_4$ receptor selectivity can be differentially modified in ribose- and base-modified analogues. Our work identifies molecules that may prove useful in pharmacologically distinguishing these receptors in complex tissues and that provide leads for rational new drug synthesis. Further evolution of molecular models for these two uracil nucleotide-activated receptors should proceed hand in hand with this novel molecule development.

## Acknowledgements

We thank Dr. Victor Marquez (NCI, Frederick, MD) for the gift of zebularine 5′-triphosphate and for helpful discussion. This research was supported in part by the Intramural Research Program of the NIH, National Institute of Diabetes and Digestive and Kidney Diseases and by NIH grants GM38213 and HL34322. Susanna Tchilibon and Pedro Besada thank the Cystic Fibrosis Foundation (Bethesda, MD) for financial support. Mass spectral measurements were carried out by Dr. John Lloyd and NMR by Wesley White (NIDDK).

## REFERENCES

[1] Seifert R, Schultz G. Involvement of pyrimidinoceptors in the regulation of cell functions by uridine and by uracil nucleotides. Trends Pharmacol Sci 1989;10:365–9.
[2] Dubyak GR, el Moatassim C. Signal transduction via P2-purinergic receptors for extracellular ATP and other nucleotides. Am J Physiol 1993;265:C577–606.
[3] Lustig KD, Shiau AK, Brake AJ, Julius D. Expression cloning of an ATP receptor from mouse neuroblastoma cells. Proc Natl Acad Sci USA 1993;90:5113–7.
[4] Communi D, Pirotton S, Parmentier M, Boeynaems JM. Cloning and functional expression of a human uridine nucleotide receptor. J Biol Chem 1995;270:30849–52.
[5] Nguyen T, Erb L, Weisman GA, Marchese A, Heng HHQ, Garrad RC, et al. Cloning, expression, and chromosomal localization of the human uridine nucleotide receptor gene. J Biol Chem 1995;270:30845–8.
[6] Chang K, Hanaoka K, Kumada M, Takuwa Y. Molecular cloning and functional analysis of a novel P2 nucleotide receptor. J Biol Chem 1995;270:26152–8.
[7] Lazarowski ER, Homolya L, Boucher RC, Harden TK. Direct demonstration of mechanically induced release of cellular UTP and its implication for uridine nucleotide receptor activation. J Biol Chem 1997;272:24348–54.
[8] Lazarowski ER, Harden TK. Quantitation of extracellular UTP using a sensitive enzymatic assay. Br J Pharmacol 1999;127:1272–8.
[9] Ralevic V, Burnstock G. Receptors for purines and pyrimidines. Pharmacol Rev 1998;50:413–92.
[10] Lazarowski ER, Boucher RC. UTP as an extracellular signaling molecule. News Physiol Sci 2001;16:1–5.
[11] Kennedy C, Qi AD, Herold CL, Harden TK, Nicholas RA. ATP, an agonist at the rat $P2Y_4$ receptor, is an antagonist at the human $P2Y_4$ receptor. Mol Pharmacol 2000;57:926–31.
[12] Bogdanov YD, Wildman SS, Clements MP, King BF, Burnstock G. Molecular cloning and characterization of rat $P2Y_4$ nucleotide receptor. Br J Pharmacol 1998;124:428–30.

[13] Webb TE, Henderson DJ, Roberts JA, Barnard EA. Molecular cloning and characterization of the rat $P2Y_4$ receptor. J Neurochem 1998;71:1348–57.
[14] Nicholas RA, Lazarowski ER, Watt WC, Li Q, Harden TK. Uridine nucleotide selectivity of three phospholipase C-activating $P_2$ receptors: identification of a UDP-selective, a UTP-selective, and an ATP- and UTP-specific receptor. Mol Pharmacol 1996;50:224–9.
[15] Harden TK, Lazarowski ER, Boucher RC. Release, metabolism and interconversion of adenine and uridine nucleotides: implications for G protein-coupled P2 receptor agonist selectivity. Trends Pharmacol Sci 1997;18:43–6.
[16] Zimmermann H. Extracellular metabolism of ATP and other nucleotides. Naunyn-Schmiedeberg's Arch Pharmacol 2000;362:299–309.
[17] Lazarowski ER, Homolya L, Boucher RC, Harden TK. Identification of an ecto-nucleoside diphosphokinase and its contribution to interconversion of P2 receptor agonists. J Biol Chem 1997;272:20402–7.
[18] Müller CE. P2 pyrimidinergic receptors and their ligands. Curr Pharmaceut Des 2002;8:2353–69.
[19] Boyer JL, Romero T, Schachter JB, Harden TK. Identification of competitive antagonists of the $P2Y_1$-receptor. Mol Pharmacol 1996;50:1323–9.
[20] Boyer JL, Adams M, Ravi RG, Jacobson KA, Harden TK. 2-Chloro-$N^6$-methyl-(*N*)-methanocarba-2′-deoxyadenosine-3′,5′-bisphosphate is a selective high affinity $P2Y_1$ receptor antagonist. Br J Pharmacol 2002;135:2004–10.
[21] Kim HS, Ohno M, Xu B, Kim HO, Choi Y, Ji XD, et al. 2-Substitution of adenine nucleotide analogues containing a bicyclo[3.1.0]hexane ring system locked in a Northern conformation: enhanced potency as $P2Y_1$ receptor antagonists. J Med Chem 2003;46:4974–87.
[22] Brown HA, Lazarowski ER, Boucher RC, Harden TK. Evidence that UTP and ATP regulate phospholipase C through a common extracellular 5′-nucleotide receptor in human airway epithelial cells. Mol Pharmacol 1991;40:648–55.
[23] Mohamadi F, Richards NGJ, Guida WC, Liskamp R, Lipton M, Caufield WC, et al. MacroModel—an integrated software system for modeling organic and bioorganic molecules using molecular mechanics. J Comput Chem 1990;11:440–67.
[24] Chang GW, Guida W, Still WC. An internal coordinate Monte-Carlo method for searching conformational space. J Am Chem Soc 1989;111:4379–86.
[25] Kolossváry I, Guida WC. Low-mode conformational search elucidated. Application to C39H80 and flexible docking of 9-deazaguanine inhibitors to PNP. J Comput Chem 1999;20:1671–84.
[26] Still WC, Tempczyk A, Hawlely RC, Hendrickson T. A general treatment of solvation for molecular mechanics. J Am Chem Soc 1990;112:6127–9.
[27] Halgren TA. MMFF. VII. Characterization of mmff94, mmff94s and other widely available force fields for conformational energies and for intermolecular interaction energies and geometries. J Comput Chem 1999;20:730–48.
[28] Fischer B, Boyer JL, Hoyle CHV. Ziganshin AU, Brizzolara AL, Knight GE, et al. Identification of potent, selective P2Y-purinoceptor agonists: structure activity relationships for 2-thioether derivatives of adenosine-5′-triphosphate. J Med Chem 1993;36:3937–46.
[29] Shaver SR, Rideout JL, Pendergast W, Douglass JG, Brown EG, Boyer JL, et al. Structure–activity relationships of dinucleotides: potent and selective agonists of P2Y receptors. Purinergic Signall 2005;1:183–91.
[30] Barchi Jr JJ, Cooney DA, Hao Z, Weinberg ZH, Taft C, Marquez VE, et al. Improved synthesis of zebularine [1-(beta-D-ribofuranosyl)-dihydropyrimidin-2-one] nucleotides as inhibitors of human deoxycytidylate deaminase. J Enzyme Inhib 1995;9:147–62.
[31] Costanzi S, Mamedova L, Gao Z-G, Jacobson KA. Architecture of P2Y nucleotide receptors: structural comparison based on sequence analysis, mutagenesis, and homology modeling. J Med Chem 2004;47:5393–404.
[32] Ohno M, Costanzi S, Kim HS, Kempeneers V, Vastmans K, Herdewijn P, et al. Nucleotide analogues containing 2-oxa-bicyclo[2.2.1]heptane and L-α-threofuranosyl ring systems: interactions with P2Y receptors. Bioorg Med Chem 2004;12:5619–30.
[33] Kim HS, Ravi RG, Marquez VE, Maddileti S, Wihlborg A-K, Erlinge D, et al. Methanocarba modification of uracil and adenine nucleotides: high potency of Northern ring conformation at $P2Y_1$, $P2Y_2$, or $P2Y_4$ and $P2Y_{11}$, but not $P2Y_6$ receptors. J Med Chem 2002;45:208–18.
[34] Erb L, Garrad R, Wang Y, Quinn T, Turner JT, Weisman GA. Site-directed mutagenesis of P2U purinoceptors. Positively charged amino acids in transmembrane helices 6 and 7 affect agonist potency and specificity. J Biol Chem 1995;270:4185–8.
[35] Pendergast W, Yerxa BR, Douglass III JG, Shaver SR, Dougherty RW, Redick CC, et al. Synthesis and P2Y receptor activity of a series of uridine dinucleoside 5′-polyphosphates. Bioorg Med Chem Lett 2001;11:157–60.
[36] Lazarowski ER, Watt WC, Stutts MJ, Brown HA, Boucher RC, Harden TK. Enzymatic synthesis of UTPγS, a potent hydrolysis resistant agonist of $P_{2U}$-purinoceptors. Br J Pharmacol 1996;17:203–9.
[37] Malmsjö M, Adner M, Harden TK, Pendergast W, Edvinsson L, Erlinge D. The stable pyrimidines UDPβS and UTPγS discriminate between the P2 receptors that mediate vascular contraction and relaxation of the rat mesenteric artery. Br J Pharmacol 2000;131:51–6.
[38] Costanzi S, Besada P, Joshi BV, Maddileti S, Mamedova L, Shin DH, et al. Human $P2Y_6$ receptor: Molecular modeling leads to the rational design of a novel agonist based on a unique conformational preference. J Med Chem, 2005; 10.1021/jm050911p.
[39] Major DT, Nahum V, Wang Y, Reiser G, Fischer B. Molecular recognition in purinergic receptor. 2. Diastereoselectivity of the h-$P2Y_1$-receptor. J Med Chem 2004;47:4405–16.